

Finite-Element Analysis of HSC. Moderately Deep Beams Using Plastic-Damage Model under Cyclic Loading

I. A. S. al-Shaarbaf

Assistant Professor

L. Kh. K. Al-Hadithy

Assistant Professor

H. M. A. Al-Bahadly

PhD. Student

Department of Civil Engineering, AL-Nahrain University, Baghdad, Iraq,

Abstract

This paper presents a numerical investigation of high-strength concrete beams moderately deep subjected to imposed inelastic cyclic deflection. Three cantilever beams having cross section of 200 x 400 mm were selected from the experimental work carried out by I-Kuang Fang, et. al. Test variables included were shear span to depth ratio, ratio of longitudinal reinforcement at top and bottom faces of the beams and loading histories. The cyclic simulation performance of the selected beams were found using the plastic-damage model for concrete developed by Lubliner and Lee & Fenves. The model adopts the concepts of fracture – energy – based damage and stiffness degradation in continuum – damage mechanics. Two damage variables, one for tensile damage and the others for compressive damage, and yield function with multiple – hardening variable are introduced to different damage states. The uniaxial strength function are factored into two parts, corresponding to the effective stress and the degradation of elastic stiffness. A simple consistent scalar degradation model is introduced to simulate the effect of damage on elastic stiffness and its recovery during crack opening and closing. It was found that the ABAQUS model accurately predicts the experimental response under cyclic loading up to the yielding of the steel bars. The prediction is less accurate at post yielding stages. This difference is due to the severe damage of the concrete in tension and compression during loading cycles. Also the prediction of the region damage within the moderately deep beams matches the experimental results. Cracks propagation (opening & closing) and stress distribution during cycles were very well predicted specially the formation of the compression struts and its development into the concrete beams. The contribution of stirrups with the plastic-hinge zone is about 30% of the latest half – cycle peak load and the developing of the plastic – hinge zone were about 150% of the beam height which were well estimated compared to the experimental results. The back bone of load-displacement curve predicted by the ABAQUS model shows a close correlation with the experimental results into the inelastic range.

Keywords : ; Crack; Cyclic loading; High concrete strength; Moderately deep beams; Numerical analysis; Plastic damage; Stiffness degradation .

التحليل بطريقة العناصر المحدده للعتبات متوسطة العمق ذات الخرسانه عالية المقاومه باستخدام أنموذج التضرر اللدن تحت تأثير الاحمال الدوريه

د. احسان علي صائب الشعرياً ف د. ليث خالد كامل الحديثي حسين محمد علي البهادلي
قسم الهندسه المدنيه / كلية الهندسه/ جامعة النهرين

الخلاصه:

تم في هذا البحث دراسة سلوك العتبات الخرسانيه المسلحه عاليه المقاومه متوسطه العمق المعرضه الى انحرافات دوريه لده. اختبرت ثلاثه نماذج من العتبات ذات مقطع بابعاد 200ملم * 400 ملم من البحث المختبر الذي اجري من قبل مجموعه I-Kuang Fang. حيث اعتبرت المعاملات التي تمثل كل من نسبة فضاء القص الى العمق و نسبة حديد التسليح الطولي في الوجه السفلي الى حديد التسليح في الوجه العلوي وكذلك أنموذج احماله متكرره متعدده الانماط لغرض الوقوف على تأثير تغييرها على سلوك هذه العتبات. اعتمد في التحليل أنموذج التضرر اللدن و الذي تم تطويره من قبل الباحثين Lee, Lubliner, Fenves و يعتمد هذا الأنموذج مبدأ أنموذج التضرر على اساس طاقة الانكسار و مبدأ تدهور جساءه العنصر في ميكانيكية تضرر الاجسام. تم تمثيل هذا التدهور بواسطة معاملين أحدهما للتضرر الحاصل نتيجة الشد والآخر لتضرر الانضغاط. اعتمدت معادله الخضوع مع عدد من معاملات التقويه بعد بلوغ الخضوع لتمثيل كافة حالات الضرر المحتمل. كانت معادله المقاومه احادية البعد ممثله بجزئين يعود احدهما الى الاجهاد المؤثر والآخر الى انحدار الجساءه المرنة. أنموذج الانحدار الذي اعتمد كان لتمثيل تأثير الضرر على الجساءه المرنة واستعادة جزء من مقدارها أثناء فتح و غلق التشققات. وجد ان استخدام الأنموذج المذكور بالاستعانه ببرنامج ABAQUS يعطي تصورا جيدا لسلوك العتبات المختارة ومدى مطابقتها مع النتائج المختبريه لغايه حد خضوع حديد التسليح. أما سلوك هذه العتبات بعد الخضوع فكان اقل دقة مما هو عليه قبل خضوع حديد التسليح وهذا التصرف يعزى الى تدهور مقاومه خرسانه قشرة المقطع مع قسم من لب المقطع مختبريا في حين ان النموذج الرياضى يبقى محتفظا ببعض الجساءه مما يؤدي الى اظهار مقاومه اعلى في مراحل تسليط الاحمال المتكرره الاخيره. اظهرت النتائج التحليلية تطابقا جيدا لمنطقه المفصل اللدن ومدى توسعها مع تكرار تسليط الاحمال وكذلك بالنسبة لتطور تشكيل التشققات وتوزيع الاجهادات داخل جسم العنصر الخرساني اضافه الى نسبة مشاركة حديد مقاومه القص في تحمل جزء من مقاومه المقطع الكلية للقص.

1-Introduction:

The main objective of this paper is to investigate the behavior of High Strength Reinforced Concrete (HSRC) moderately deep beams subjected to cyclic loading. Material non-linearity of concrete due to yielding, cracking, plastic deformation, crushing of concrete and yielding of reinforcement are considered. The behavior of deep beams under cyclic loading is an important aspect in seismic resistant design of structures. Deep beams are required to withstand very large shear forces, while also possessing sufficient ductility to dissipate the energy produced during the cyclic loading event. The load-deformation curves, plastic-hinge, region damage and stirrups contribution within the plastic-hinge using Lubliner et al [1] and Lee & Fenves [2] plastic damage models have been conducted to three cantilever moderately deep beams. The examples have been chosen in order to demonstrate the applicability of the selected plastic damage model by comparing the predicted response to the behavior that observed experimentally

2-Finite element model :

The main task is to model the HSC. moderately deep beams in ABAQUS; which is powerful numerical tool used for component and system modeling and finds its application in various fields; using the material models and damage density parameters. The moderately HSC deep beams were decided to be modeled in a three dimensional analysis which requires greater computational effort than two dimensional analysis in order to simulate the behavior of plane dimensions. The stress and the crack propagation across the section width was assumed to be taken into consideration. Quadratic geometric order element are used as the effect of bending is considerable in the solver option. The evolution and distribution of the crack pattern and the possible modes of failure are to be obtained from this model. The integration rules which have been used in this work are,

- a- The 8(2x2x2) Gauss-quadrature integration rule
- b- The 27(3x3x3) Gauss-quadrature integration rule

Reinforcement bars have been simulated as axial members embedded within the concrete element. Perfect bond is assumed to occur between the steel and concrete .

3-Material model :

The material model used in the present work is suitable for concrete under cyclic loading. The behavior of concrete in compression and tension is proposed by Aslani and Jowkarmeimandi [3]. The proposed compressive envelope curve is based on the model of Carreira and Chu (1985) [4], as given by Equations (1)to(9) (the equations presented in this study are in metric units).

$$\sigma_c/f_c = n (\varepsilon_c / \varepsilon_c') / (n-1+(\varepsilon_c / \varepsilon_c')^n) \quad (1)$$

$$n= n_1=[1.02-1.17(E_{sec} / E_c)]^{0.74} \text{ if } \varepsilon_c \leq \varepsilon_c' \quad (2)$$

$$n= n_2= n_1+(a+28b) \quad \text{if } \varepsilon_c \geq \varepsilon_c' \quad (3)$$

where,

$$a= 3.5(12.4-1.66 \times 10^{-2} f_c')^{-0.46} \quad (4)$$

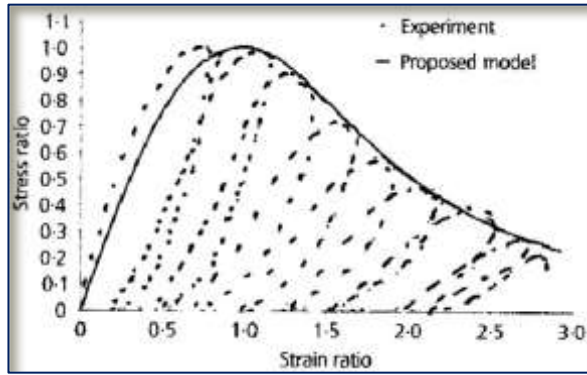
$$b=0.83 \exp(-911/ f_c') \quad (5)$$

$$E_{sec}= f_c' / \varepsilon_c \quad (6)$$

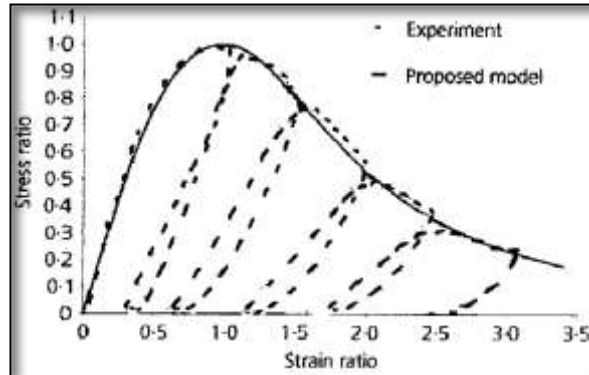
$$E_c= 3320(f_c')^{0.5}+6900 \quad (7)$$

$$\varepsilon_c=(f_c' / E_c)(r/ (r-1)) \quad (8)$$

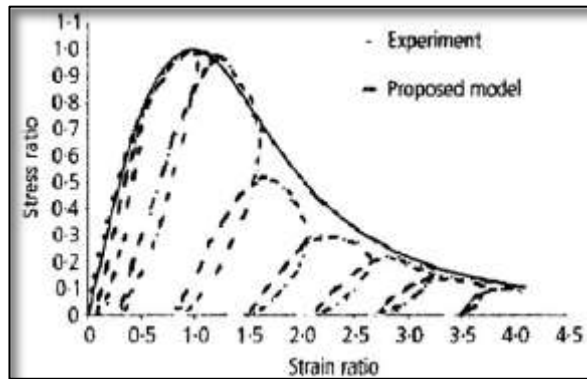
$$r = (f_c'/17)+0.8 \quad (9)$$



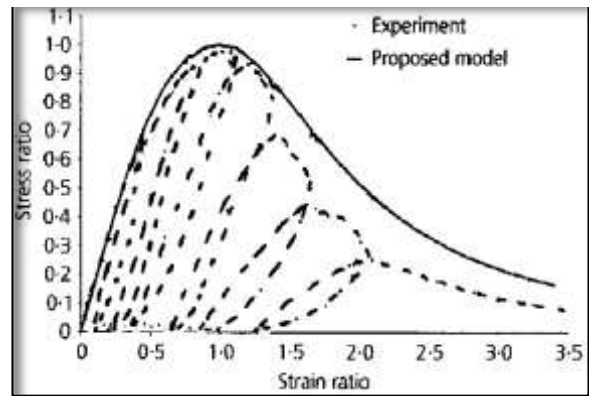
Figure(1).Comparison of experimental data of Sinha et al.(1964) [5] with proposed model.



Figure(2).Comparison of experimental data of Okamoto et al.(1976) [6] with proposed model



Figure(3).Comparison of experimental data of Tanigawa and Uchida(1979) [7] with proposed model



Figure(4).Comparison of experimental data of Bahn and Hsu(1998) [8] with proposed model.

σ_c is the concrete stress in general, f_c' is the specified concrete compressive strength, n is the material parameter that depends on the shape of the stress-strain curve, n_1 is the modified material parameter at ascending branch, n_2 is the modified material parameter at descending branch, ϵ_c is the axial concrete strain in general, ϵ_c' is the tensile strain corresponding to tensile strength, E_c is the tangent modulus of elasticity, E_{sec} is the secant modulus of elasticity.

The proposed tensile envelope curve of stress-strain model for concrete under cyclic loading is given by equation (10) which is a very simple model .

$$\left\{ \begin{array}{l} \sigma = \epsilon_c E_c \text{ if } \epsilon_c \leq \epsilon_{ct}' \text{ and} \\ \sigma = f_c' (\epsilon_{ct}' / \epsilon_c)^{0.85} \text{ if } \epsilon_c \geq \epsilon_{ct}' \end{array} \right\} \quad (10)$$

where, ϵ_{ct}' is the tensile concrete strain in general .

For repeated compressive loading, several uniaxial cyclic test results have been compared with prediction obtained by means of model presented. These tests cover several concrete strength value and variety of cyclic loading histories. In the case of cyclic compression, results from works performed by Sinha et al.(1964) [5], Okamoto et al.(1976) [6], Tanigawa and Uchida(1979) [7]

and Bahn and Hsu (1998) [8] were considered. Figures (1)to(4) show these experimental tests for cyclic compressive loading compared with proposed model.

For repeated tensile cyclic loading; in the case of cyclic tension and cyclic tension with small incursions in compression, the model is compared with test results reported by Reinhardt(1984) [9]. (Fig.(5)) and Yankelevsky and Rrinhardt(1987) [10]. (Fig.(6)).

In both cases the present model shows satisfactory agreement with the experimental results [3].

The reinforcing steel bars are simulated using the model developed by Manegotto and Pinto(1973) [11], described by the equation (11),

$$f_s = (E_s \epsilon_s / (1 + (E_s \epsilon_s / f_y)^{20})^{0.05}) + (f_{su} - f_y) * [((1 - (\epsilon_{su} - \epsilon_s)^p / (\epsilon_{su} - \epsilon_{sh}))^{20p} + (\epsilon_{su} - \epsilon_s)^{20p})^{0.05}] \quad (11)$$

where, $p = E_{sh} ((\epsilon_{su} - \epsilon_{sh}) / (f_{su} - f_y))$,

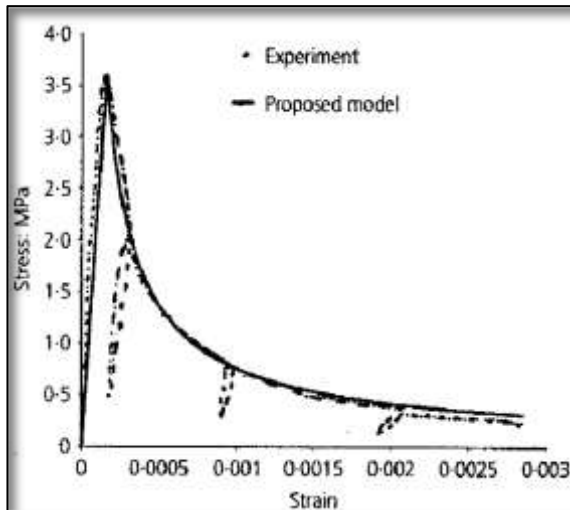
E_s is the Young Modulus in MPa,

f_y is the yield stress of the steel in MPa,

f_s is the stress in the reinforcing steel in MPa,

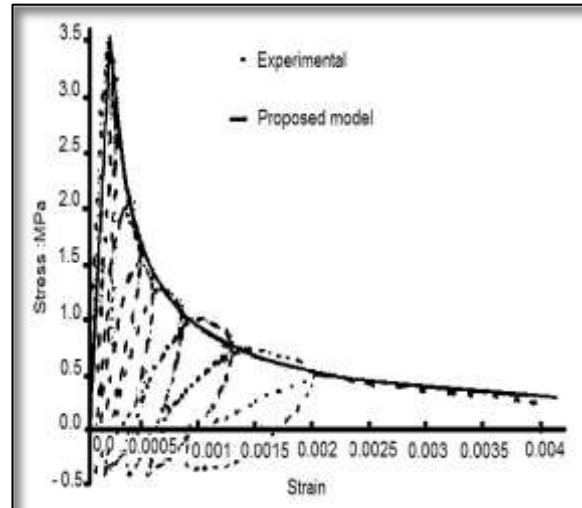
ϵ_s is the strain in the steel,

f_{su} is the ultimate strength of the steel in MPa,



ϵ_{su} is the ultimate strain in the steel and

Figure(5).Comparison of experimental data of Reinhardt(1984) [9]with proposed model



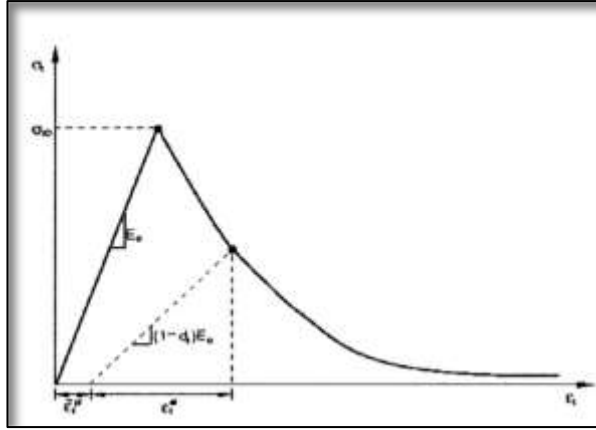
ϵ_{sh} is the hardening strain in steel .

Figure(6).Comparison of experimental data of Yankelevsky and Reihardt (1987) [10] with proposed model

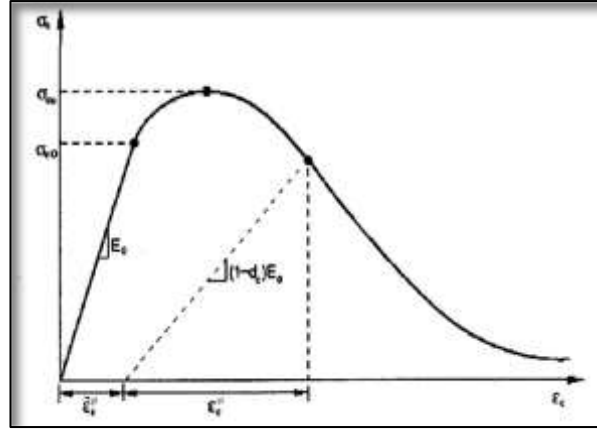
4-Modeling techniques :

ABAQUS has different models to represent the concrete and steel. The experimental data used in this study had loading that is cyclic in nature. Therefore, the concrete model should accommodate the corresponding actions such as recovery of stiffness on reversal of loading and cracked behavior of concrete. The concrete damage plasticity model is seen as the best option to do this as it incooperates these characteristics. The concrete damaged plasticity is based on the plasticity model proposed by Lubliner et al.(1989) [1] and Lee and Fenves (1998) [2] . The formulation features of the model are discussed elsewhere [12].

The stress-strain behavior in tension and compression obtained using the formulation presented in reference [12] is shown in Fig.(7) and (8), respectively.



Figure(7). Concrete behavior in tension [12].



Figure(8). Concrete behavior in compression [12].

Under uniaxial cyclic loading the degradation behavior involves the opening and closing of previously formed microcracks. It is observed through experimental work that there is a recovery of elastic stiffness as the load changes, this effect is called "unilateral effect". The effect is seen in a greater degree when the load changes from tension to compression. The elastic modulus of material is expressed in terms of the scalar degradation as,

$$E = (1-d) E_0 \quad (11)$$

where, E_0 is the initial (undamaged) modulus of material.

This expression holds both in tensile and compressive sides of the cycle. The stiffness reduction variables and the damage variables d_t and d_c are assumed as,

$$(1-d) = (1-s_t d_t) (1-s_c d_c) \quad 0 \leq \epsilon_c, \epsilon_t \leq 1 \quad (12)$$

where, s_t and s_c are functions of the stress and are introduced to represent stiffness recovery effects defined as,

$$s_t = 1 - w_t r^*(\bar{\sigma}_{11}) \quad 0 \leq w_t \leq 1 \quad (13)$$

$$s_c = 1 - w_c (1 - r^*(\bar{\sigma}_{11})) \quad 0 \leq w_c \leq 1 \quad (14)$$

$$\text{Where, } r^*(\bar{\sigma}_{11}) = 1 \text{ if } (\bar{\sigma}_{11}) > 0 \quad (15)$$

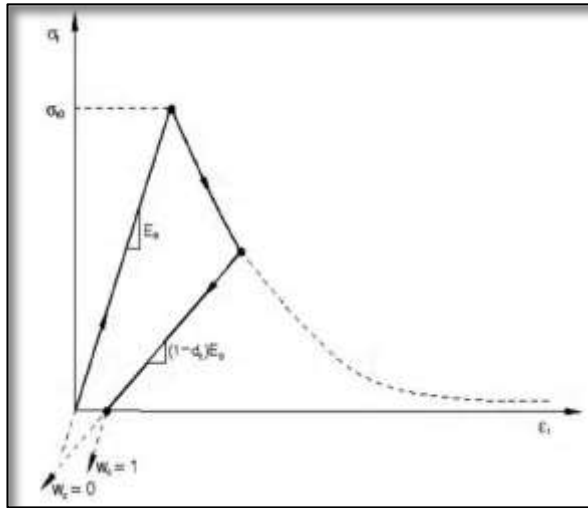
$$r^*(\bar{\sigma}_{11}) = 0 \text{ if } (\bar{\sigma}_{11}) < 0$$

The weight factors w_t and w_c which are assumed to be as material properties, control the recovery of the tensile and compressive stiffness upon load reversal. The effect of the compression stiffness

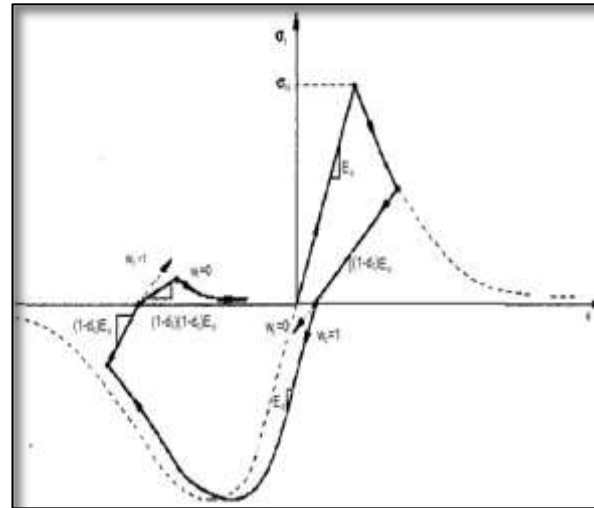
recovery factor w_c on the behavior of concrete is shown in Fig.(9). The model assumes that the elastic stiffness degradation to be isotropic and characterized as,

$$D^e = (1-d) D^e_0 \quad (16)$$

With d being the scalar degradation variable as defined for uniaxial cyclic loading. The uniaxial load cycle is shown in Fig.(10).The plastic damage concrete model uses a yield condition based on the yield proposed by Lubliner et al.(1989) [1] and incorporates the modification proposed by Lee and Fenves (1998)[2] to account for different strength evolution under tension and compression .



Figure(9).Effect of compression stiffness recovery factor w_c [12]

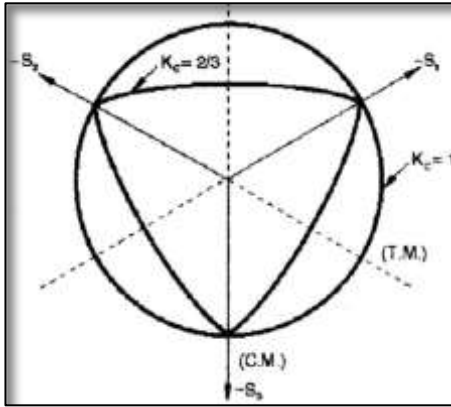


Figure(10).Uniaxial load cycle (tension-compression-tension) [12].

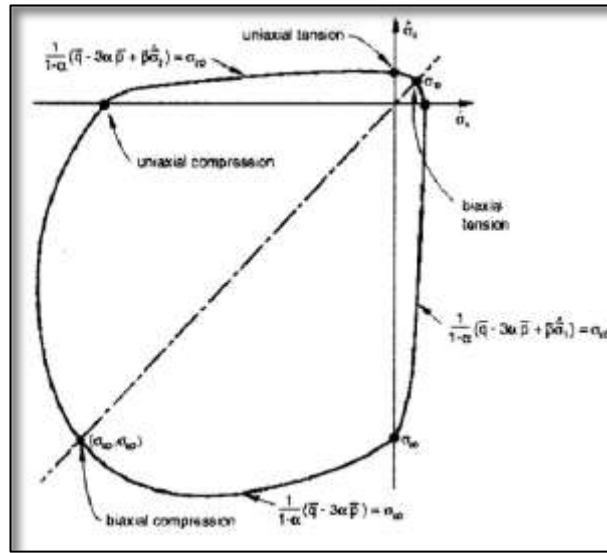
The yield function formulation is described in details in references [1], [2] and [12]. The surface obtained for deviatoric plane and in plane stress formulation are shown in Fig.(11) and (12) respectively.

ABAQUS requires the following input for computing the damage in concrete:

- Dilation angle; ψ ; the $\psi=36^\circ$ is used .
- Flow potential eccentricity ; ε ; the $\varepsilon=0.1$ is used .
- $\sigma_{b0} / \sigma_{c0}$ is the ratio of initial equibiaxial compressive yield stress to initial uniaxial compressive yield stress . The ratio of 1.16 is used
- K_c , is the ratio of the second stress invariant on the tensile meridian, $q(TM)$, to that on the compressive meridian, $q(TM)$. The default of $2/3$ is used.
- Viscosity parameter; μ ; is used for visco-plastic regularization of the concrete constitutive equation, in ABAQUS standard analysis a default value of $0.0 (c^\circ)$ is used .



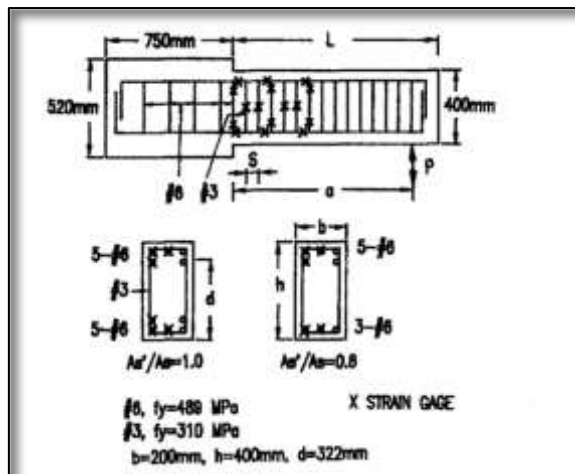
Figure(11).Yield surface of deviatoric plane [12]



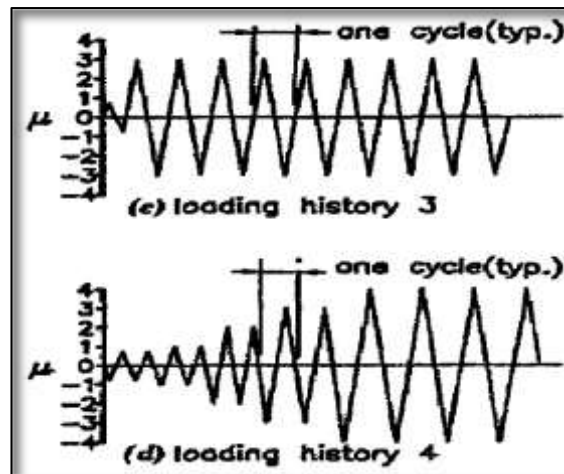
Figure(12).Yield surface in plane stress [12]

5-Numerical examples :

In order to investigate the behavior HSRC moderately deep beams subjected to cyclic loading, three reinforced concrete cantilever beams selected from experimental work conducted by Fang et al.[13] have been analyzed. For the selected beams, the material properties, the additional material parameters and the (bottom to top) longitudinal reinforcement ratio (A_S/A_S), loading history and shear span to effective depth ratio are shown in Table(1) . The three beams were 200mm in width by 400mm in depth . Details of test specimens were shown in Fig.(13) .



Figure(13).Details of test specimens



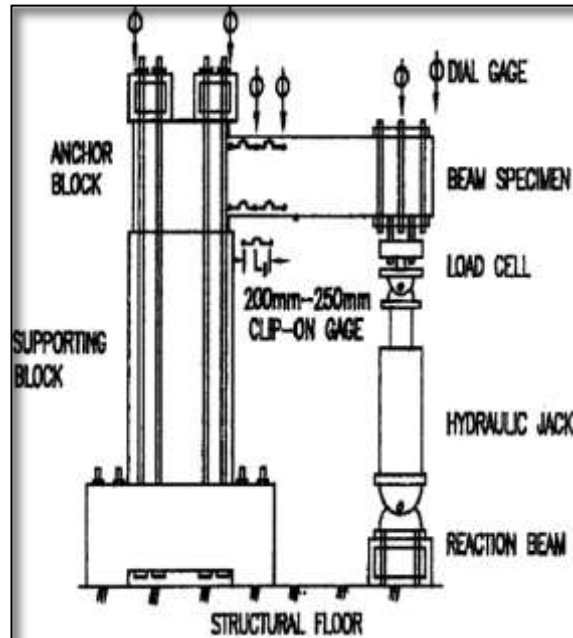
Figure(14).Loading histories used for the analysis

The loading history for the selected beams are shown in Fig.(14). μ is defined here as the ratio of load-point deflection to the first yield displacement at the same location. The ratio μ was determined when the strain-gage readings of the longitudinal steel at fixed end reaches the first yield strain through monitoring the data scanned during the test.

6-Experimental test procedure :

As shown in Fig.(15), the anchor block of the specimen was tied down by two box steel beams to provide the fixed end restraints. The load was supplied by a simplex hydraulic jack near the tip of the beam. To monitor the flexural deformation within the plastic-hinge zone, clip-on gages were installed on steel studs, which were welded at the appropriate location of longitudinal reinforcement before the casting of concrete . Strain gages were mounted on longitudinal and transverse reinforcement as shown in Fig(13).[13].

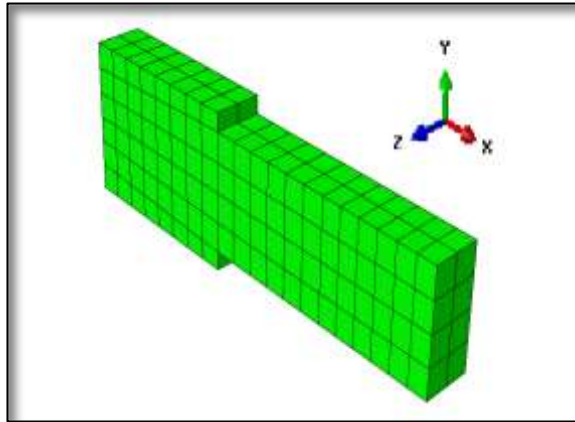
Figure(15).Test setup used for the experimental tests. [13]



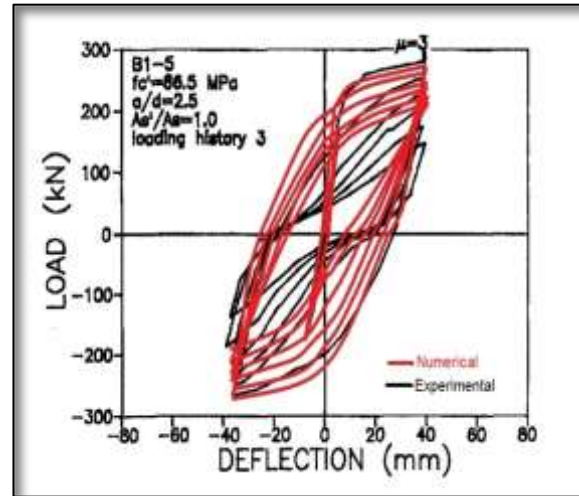
7-Numerical results of beam B1-5 :

Effect of integration rule and mesh study for concrete element have been conducted to B1-5 . Mesh arrangement shown in Fig.(16-a) has been chosen after using varieties of mesh arrangements for the finite element analysis . The 27(3x3x3) Gauss-quadrature integration rule was used from the two types of integration rules mentioned before, in conjunction with the mesh arrangement selected above for the three tested beams. The experimental and the numerical load-displacement back bone curves obtained for beam B1-5 is shown in Fig. (16-b). The finite element solution is in good agreement with the experimental result up to the yielding of the steel bars. The prediction is less accurate at post yielding stages. It was also shown that the numerical results give predicted loads greater than the experimental loads at latest cycles; this behavior is seen because experimentally the concrete cover and some of concrete core of the beam have been totally damaged during test, but mathematically they are exists with little margin of stiffness causes such behavior. In order to verify this behavior, another analysis has been carried out with the removal of top and bottom concrete covers. The analysis results obtained were in good correlation with those obtained experimentally specially at the latest cycles of loading as shown in Fig.(17).

ABAQUS model accurately predicts cracks propagation (opening and closing) during loading cycles in tension and compression faces of the beam; Fig.(18) shows the crack pattern at the ends of the halves of the first three cycles of loading in beam B1-5.



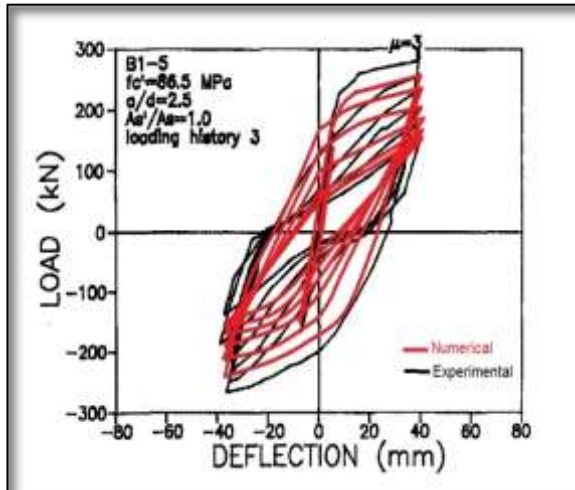
(a)



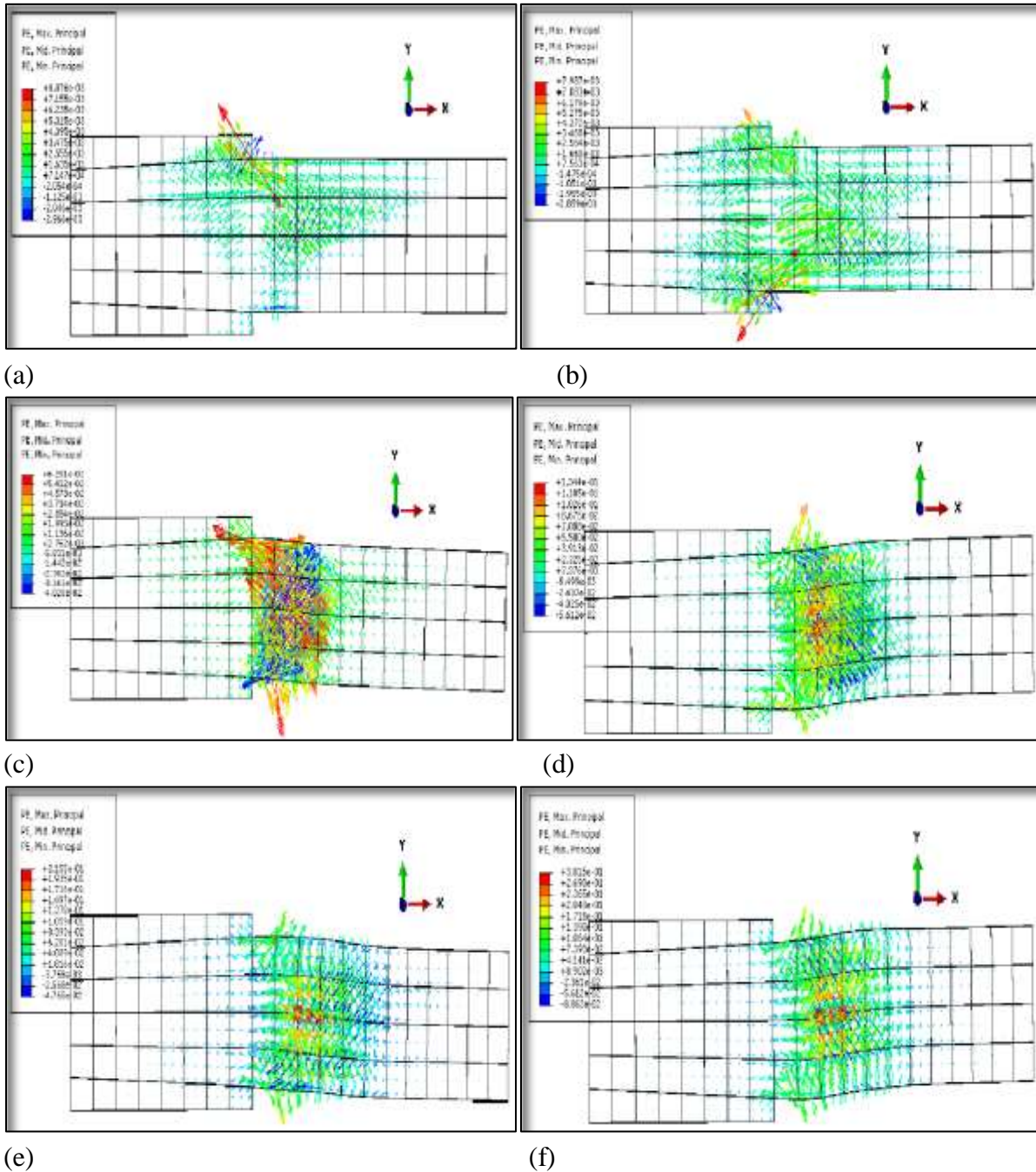
(b)

Figure(16) a) Mesh arrangement of B1-5

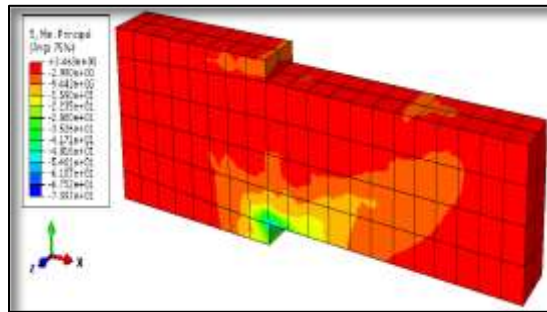
b) Numerical and experimental load-displacement back-bone curve of B1-5



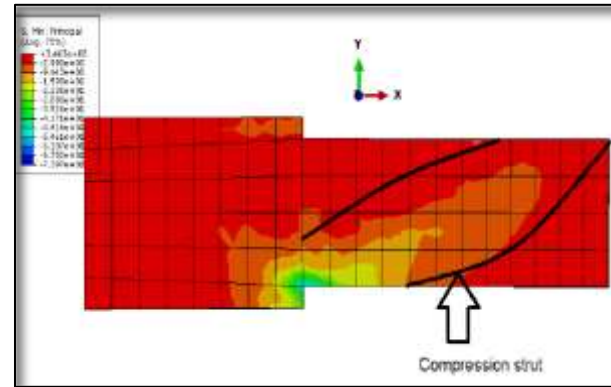
Figure(17), Numerical and experimental load-displacement back-bone curve of B1-5 after removal of concrete beam covers.



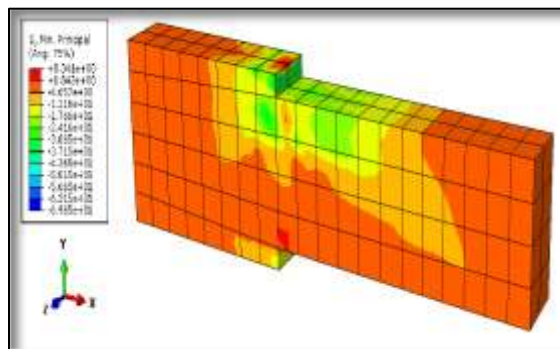
Figure(18).Beam B1-5 crack pattern at, a) 1st half of cycle (1), b) 2nd half of cycle (1), c) 1st half of cycle (2), d) 2nd half of cycle (2), e) 1st half of cycle (3), f) 2nd half of cycle (3).



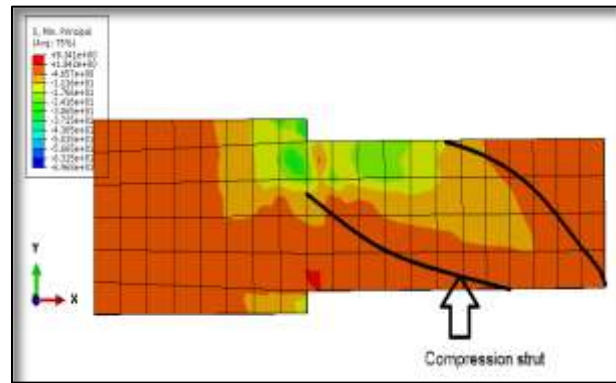
(a)



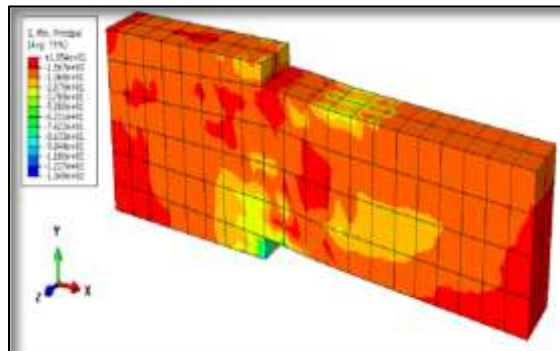
(b)



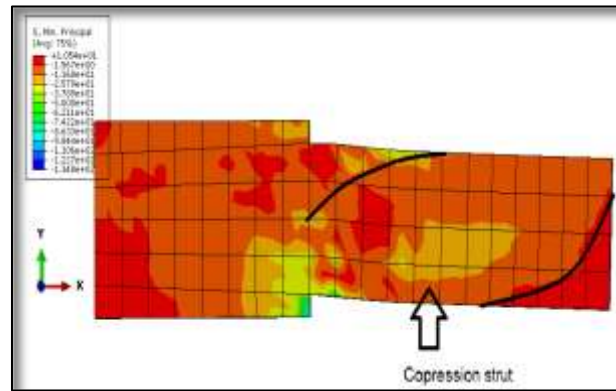
(c)



(d)



(e)



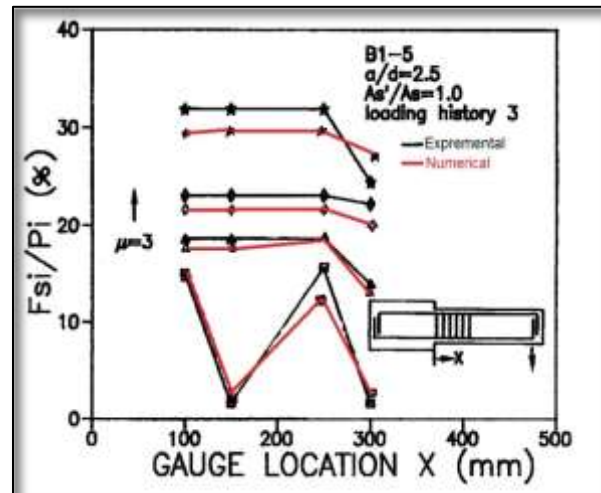
(f)

Figure(19).Beam B1-5 compression struts formation at, a) 1st half of cycle (1), b) 1st half of cycle (1) side view c) 2nd half of cycle (1), d) 2nd half of cycle (1) side view , e) 1st half of cycle (2) f) 1st half of cycle (2) side view .

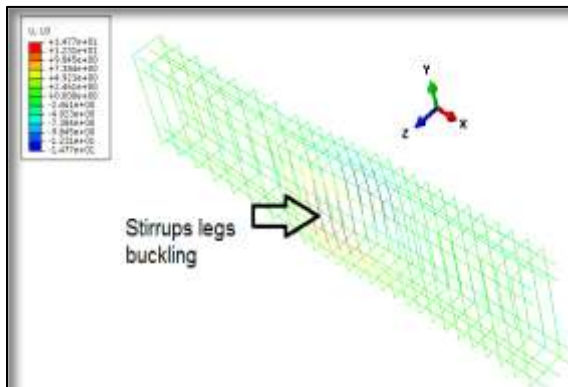
Table(1).Properties of selected deep beams [5].

| specimen | f_c (MPa) | a/d | Shear span(a)mm | Loading history | A_S/A_S | Stirrups spacing(s)mm | Beam length(L)mm |
|----------|-------------|-----|-----------------|-----------------|-----------|-----------------------|------------------|
| B1-3 | 86.5 | 2.5 | 850 | 3 | 0.6 | 50 | 1050 |
| B1-5 | 86.5 | 2.5 | 850 | 3 | 1.0 | 50 | 1050 |
| B3-3 | 85.7 | 3.5 | 1150 | 4 | 0.6 | 70 | 1350 |

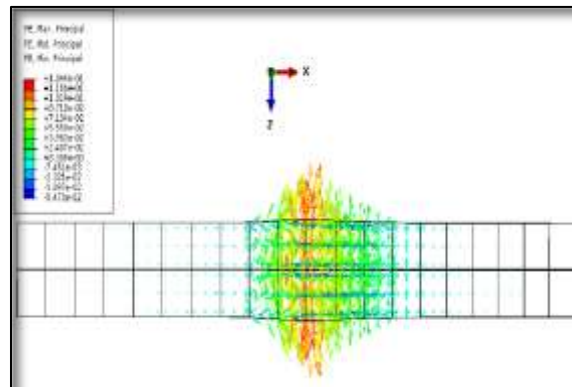
Also the stress distribution during loading cycles was well predicted specially the formation of the compression struts and its development into concrete body as shown in Fig.(19). The width of compression strut is increased as the load cycle increases. This behavior is attributed to the increasing damage in concrete body which causes a decrease in the net area available to withstand the compression forces; so the forces will be redistributed over the areas which adjacent to previous compression struts areas. The contribution of stirrups in HSC beams subjected to sever cyclic loading is helpful in visualizing the role of stirrups. The numerical results of stirrups contribution within the plastic hinge region is shown in Fig.(20). The ratio of shear forces (F_{si}) contributed by individual gaged stirrup within the hinge region to the peak load (P_i) in that half cycle is indicated. The numerical and experimental results show that the contribution of stirrups with the plastic hinge zone was about 30% of the latest half cycle peak load with small deviation between the numerical and experimental results. The use of three dimensional model shows the account for the proper confinement and the transverse steel behavior, Fig.(21-a). The effect of cracks opening in the direction of the width of the beam (z-direction) is clearly shown in Fig.(21-b) causing lateral displacement to push the stirrups legs to the outer direction (buckling in the stirrups legs).



Figure(20). Numerical and experimental results of stirrups contribution within plastic hinge zone



(a)

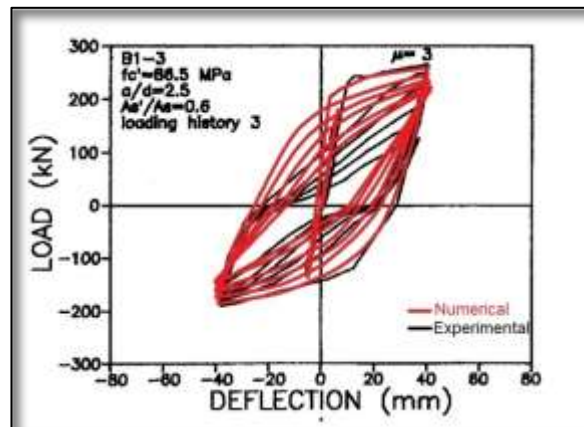


(b)

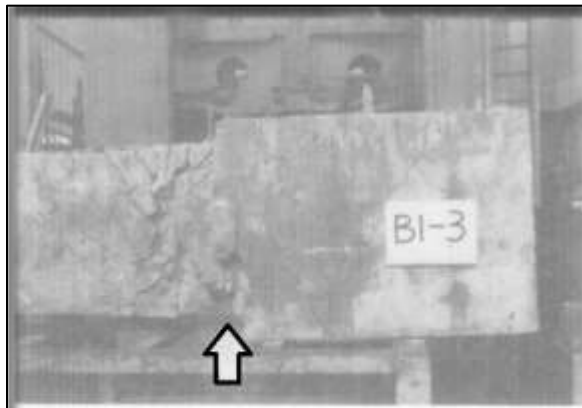
Figure(21). a) Transverse steel buckling within plastic hinge zone b) Cracks propagation in (z-direction) of beam within plastic hinge zone

8-Numerical results of beam B1-3 :

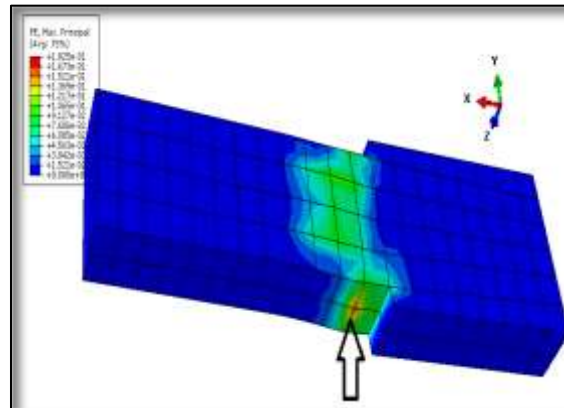
This beam is similar to beam B1-5 except that the longitudinal steel ratio (A_s'/A_s) of the bottom steel was 0.6. The numerical results of load-displacement back bone curve predicted by ABAQUS model shows a close correlation with experimental results up to yielding of reinforcement bars as shown in beam B1-5. Also the response is less accurate at post yielding stages as illustrated in Fig.(22) and the damaged region within the plastic hinge zone which was severely damaged as shown in experimental work specially at the bottom face (face of less steel ratio), Fig.(23).



Figure(22). Numerical and experimental load deformation curve of beam B1-3 .



(a)

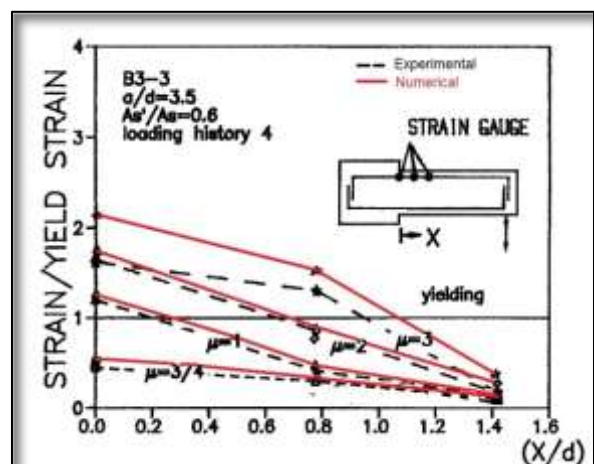


(b)

Figure(23). a) Experimental damaged region , b) Numerical damaged region .

9-Numerical results of beam B3-3 :

Beam B3-3 was chosen to study the development of the plastic hinge zone as the load cycles applied . The plastic hinge zone considered in the study was monitored by observing the strain gage readings at various gaged locations of the longitudinal reinforcement. Experimentally the gage readings were lost during the stages of large inelastic deformation . The observed shear sliding of beam near the anchor block was used to locate the plastic hinge zone Fig.(24) shows the



Figure(24). Numerical and experimental developing of plastic hinge of beam B3-3

numerical and experimental development of plastic hinge zone . It is concluded that the half length of the plastic hinge in HSC moderately deep beams is about three fourths the effective depth of the beam which is quit close to that of experimental results .

10-Conclusions :

Based on numerical analyses carried out obtained through the present research, the following conclusions can be drawn.

- 1- The finite element and the material models used in the present research can adequately simulate the behavior of HSC moderately deep beams under cyclic loading
- 2- The pre-yield behavior predicted is in good match with the experimental results, while the post yielding numerical results do not match as closely .
- 3- The three dimensional model adopted in this study clearly predicts the behavior of moderately deep beams and improves the behavior to account for the proper confinement and transverse steel role throughout the entire stages of analysis compared with 2-D analysis .
- 4- The numerical tests revealed that the ABAQUS model ;
 - a-Can safely predicts the behavior of HSC moderately deep beams under cyclic loading.
 - b-Predicted the experimental response accurately under cyclic loading up to yielding of steel bars. However, the predicted results were less accurate during the inelastic range.
 - c-Predicts the back bone curve with acceptable correlation of experimental results into the inelastic range.
 - d-Can clearly predict the region of damage within the moderately deep beams.
 - e- Very well predicted the numerical results of cracking patterns and stress distribution during cyclic loading.
- 5- The numerical results show that the contribution of stirrups within the plastic hinge zone in good agreements with the experimental results. It is found that the accuracy is within 30% for the latest half cycle peak load .
- 6- According to the finite element results, the development of plastic hinge zone was found to be about 150% of the beam height which were well estimated compared to the experimental results .

11-References :

- [1] Lubliner,J., Oliver,J., Oller,S. and Onate,E. (1989)."A plastic damage model for concrete ." Int. J. Solids and Struc., 25(3), 299-326
- [2] Lee,J., and Fenves,G.L. (1998)."Plastic damage model for cyclic loading of concrete structure." J. of Engineering Mechanics 1998. 124: 892-900.
- [3] Aslani,F., and Jowkarmeimandi, R.(2012) "Stress-strain model for concrete under cyclic loading." Magazine of Conc. Research., 2012, 64(8), 673-685
- [4] Carreira DJ and Chu KH (1985) Stress–strain relationship for plain concrete in compression. ACI Journal 82(6): 797–804.
- [5] Sinha BP, Gerstle KH and Tulin LG (1964) Stress–strain relations for concrete under cyclic loading. ACI Structural Journal 61(2): 195–211.

- [6] Okamoto S, Shiomi S and Yamabe K (1976) Earthquake resistance of prestressed concrete structures. Proceedings of Annual Architectural Institute of Japan (AIJ) Convention, Japan, pp. 1251–1252
- [7] Tanigawa DC and Uchida Y (1979) Hysteretic characteristics of concrete in the domain of high compressive strain. Proceedings of Annual Architectural Institute of Japan (AIJ) Convention, Japan, pp. 449–450.
- [8] Bahn BY and Hsu TTC (1998) Stress–strain behavior of concrete under cyclic loading. *ACI Material Journal* 95(2): 178–193.
- [9] Reinhardt HW (1984) Fracture mechanics of an elastic softening material like concrete. *Heron* 29(2): 1–42.
- [10] Yankelevsky DZ and Reinhardt HW (1987) Response of plain concrete to cyclic tension. *ACI Material Journal* 84(5): 365– 373.
- [11] Menegotto, M., and Pinto, P. E. (1973). " Method of analysis for cyclically loaded reinforced concrete plane frames including changes in geometry and non-elastic behavior of elements under combined normal force and bending." *IABSE Symposium on the Resistance and Ultimate Deformability of Structures Acted on by Well-defined Repeated Loads*, Lisbon Portugal, 15-22.
- [12] ABAQUS (2010) Abaqus/CAE6.10-1 User Manual, Inc.,<http://nmt.blogspot.org/2080/v6.10/books/stm/ch04s05ath120.html>
- [13] Fang,I.K.,Yen,S.,Wang,Ch. And Hong, K., "Cyclic behavior of moderately deep HSC. beams ."J. of Struc. Engineering, vol. 119, No.9, September, 1993, 2573